

CFD MODELLING OF THE RADIATION AND CONVECTION LOSSES IN THE M TSA RECEIVER

Dong CHEN¹, Yunlong LIU¹, Regano BENITO² and Wes STEIN²

¹ CSIRO Division of Manufacturing and Infrastructure Technology, Highett, Victoria 3190, AUSTRALIA

² CSIRO Division of Energy Technology, Mayfield West, Newcastle, NSW 2300, AUSTRALIA

ABSTRACT

CFD investigation of the radiation and convection losses for a cavity solar receiver at the CSIRO National Solar Energy Centre was carried out using Fire Dynamics Simulator (FDS). In general, if there is no wind effect, the convective heat losses through the aperture are between 5% to 15% of the radiative losses with this ratio increasing for larger apertures. Modelling results suggest that with no wind effect, thermal efficiency is in the range of around 71-85% for a receiver with 0.4m × 0.4m absorber and 0.4m × 0.4m aperture operated between 700 and 900 °C with a total absorbed energy of 25 kW. Preliminary analysis indicated that for a small cavity receiver, ambient wind may have a substantial impact on the overall heat loss from the receiver. In order to achieve high thermal efficiency, it is suggested that a small receiver should have wind guards installed to reduce the wind effect.

NOMENCLATURE

f	external force vector (excluding gravity)
g	acceleration vector of gravity
<i>h</i>	enthalpy
<i>k</i>	thermal conductivity
<i>p</i>	pressure
Pr	Prandtl number
q_r	radiative heat flux vector
Re	Reynolds number
<i>T</i>	temperature
<i>t</i>	time
u	velocity vector
<i>V_a</i>	average influx velocity through the aperture
<i>V_b</i>	average influx velocity through aperture induced by buoyancy only
<i>V_w</i>	wind speed

Symbol

ρ	density
μ	dynamic viscosity
τ	viscous stress tensor

INTRODUCTION

The National Solar Energy Centre (NSEC), which is based at CSIRO's Energy Centre in Newcastle, has as its flagship project a Solar Tower Array (Figure 1). With all of its 200 mirrors in operation, the array can concentrate more than 500 kW of solar energy and is capable of achieving peak temperatures of over 1000 °C. This high temperature energy source can be used for a variety of

applications such as, thermochemical (eg. SolarGas™ production) reaction, steam production, desalination, concentrating sunlight onto solar cells (PV), water splitting etc.

SCRR
 Location

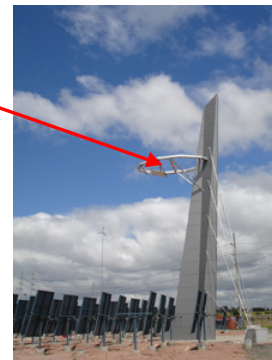


Figure 1 The Solar Tower Array at Newcastle Energy Centre.

Prior to this project, a solar dish and cavity receiver was built and tested at Lucas Heights, Sydney. The new Solar Tower Array project at Newcastle follows on from the successful Lucas Heights work. CSIRO is in the process of installing a solar cavity receiver and reactor (SCRR) at the focal point of the array for research and development of the SolarGas™ production technology. As shown in Figure 2, the reactor on the tower uses concentrated solar energy to react water and natural gas over a catalyst. The resulting SolarGas™ (3H₂ + CO) comprises 26 percent more energy than the original natural gas - this increased energy content is directly attributable to concentrated solar energy.

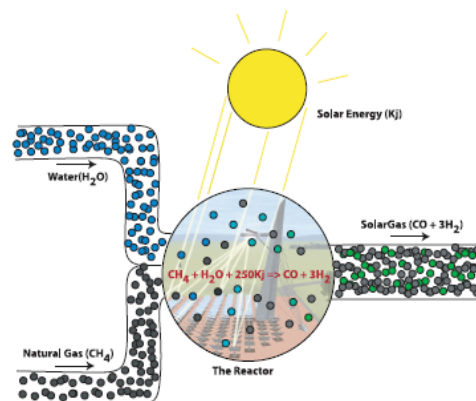


Figure 2 The SolarGas™ technology.

In order to maximize solar energy efficiency of the SCRR, the radiation and convection losses in the solar cavity receiver need to be understood and should be minimised. Several researchers have investigated the radiative and convective losses from cavity receivers. Clausing (1981) proposed an analytical model for large cubical receivers for the convective loss through the aperture due to buoyancy and wind effects. The model was further modified and verified by the experimental data of a 2.7m square aperture receiver (Clausing, 1983). Koenig and Marvin (1981) and Stine and McDonald (1989) proposed empirical correlations for convective heat losses which includes the effect of inclination angle and aperture size. Leibfried *et al* (1995) developed correlations for convective losses based on their experimental studies using electrically heated spherical and hemispherical receivers with apertures ranging from 60 to 195mm in diameter.

Taumoefolau and Lovegrove (2002) and Paitoonsurikarn and Lovegrove (2002) experimentally and numerically investigated the natural convective losses from a 70 mm cylinder receiver with cavity temperatures ranging from 350 to 500 °C. It was reported that the experimental and numerical results obtained are in good qualitative agreement with those predicted by various correlations proposed by previous researchers. The Clausing (1981) correlation shows the closest prediction despite its original use for larger-scale central receivers. It should be noted that these correlations were developed on relatively few geometries and limited operating conditions. Their application to different geometries and operating conditions requires caution. In this study, a CFD investigation has been carried out to improve understanding and estimation of the radiative and convective losses from solar cavity receivers.

CFD MODELLING

A CFD package Fire Dynamics Simulator (FDS) (McGrattan *et al*, 2005) was used for this study. FDS is a computational fluid dynamics (CFD) model for modeling buoyancy-driven fluid flow. The model numerically solves the Navier-Stokes equations for low-speed, thermally-driven flow with emphasis on heat and mass transport. The partial derivatives of the conservation equations of mass, momentum and energy are approximated as finite differences, and the solution is updated in time on a three-dimensional, rectilinear grid.

Turbulence is treated by means of the Smagorinsky form of the large eddy simulation (LES), in which the large-scale eddies are computed directly and sub-grid scale dissipative processes are modeled.

FDS solves the basic conservation of mass, momentum and energy equations for a thermally-expandable, multi-component mixture of ideal gases. The basic sets of equations are presented here:

Conservation of mass:

$$\frac{\partial \rho}{\partial t} + \nabla \cdot \rho \mathbf{u} = 0 \quad (1)$$

Conservation of momentum:

$$\rho \left(\frac{\partial \mathbf{u}}{\partial t} + (\mathbf{u} \cdot \nabla) \mathbf{u} \right) + \nabla p = \rho \mathbf{g} + \mathbf{f} + \nabla \cdot \boldsymbol{\tau} \quad (2)$$

Conservation of energy:

$$\frac{\partial}{\partial t} (\rho h) + \nabla \cdot \rho h \mathbf{u} = \frac{Dp}{Dt} - \nabla \cdot \mathbf{q}_r + \nabla \cdot \kappa \nabla T \quad (3)$$

Radiative heat transfer is included in the model via the solution of the radiation transport equation for a non-scattering gray gas. The equation is solved using a technique similar to finite volume methods for convective transport, thus the name given to it is the Finite Volume Method (FVM). Using 100 discrete angles, the finite volume solver requires about 15% of the total CPU time of a calculation, a modest cost given the complexity of the radiation heat transfer.

SCRR MODEL DESCRIPTION AND ASSUMPTIONS

As FDS uses rectilinear grids, rectangular receiver designs have been modeled in this study. Figure 3(a) and (b) show the model of a rectangular receiver which is located at the middle of a large cubic computational domain.

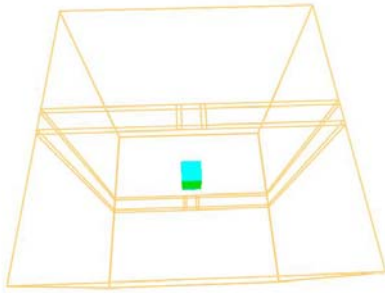
Table 1 lists the different receiver geometries simulated in this study. The large outer domain is a 6.2 m cubic with all six boundaries fully open to the ambient conditions. For all the cases modelled in this study, the receiver is located at the centre of this large computational domain as shown in Figure 3. The following assumptions were made in this study:

- The absorber is maintained at a given constant temperature.
- Ambient wind speed is zero.
- Ambient temperature is 21 °C.
- The whole system is at ambient temperature at the start of the simulation.
- All the receiver walls are thermally insulated with no conductive heat losses.
- The normal of the receiver aperture is inclined 17 degree from the vertical on the tower array.
- The emissivity of all the walls is assumed to be 0.7.

SIMULATION RESULTS

An SGI Altix high performance computer was used in all simulations. In order to take the advantage of this multi-processor computer, the computational domain has been divided into 7 inter-connected zones and the modelling was carried out with 7 processors running parallel.

A sensitivity study on the grid size indicated that around one million grids are needed to get grid-size independent results. A total of 1.1 million grids were used in each case study. Time step size was automatically adjusted so that the Courant-Friedrichs-Lewy (CFL) condition was satisfied (McGrattan *et al*, 2005). The averaged time step used in the present computation was around 0.02s. Enlargement of the computational domain from 6.2 m cubic to 10 m cubic was found to have no impact on the simulated results of radiative and convective losses. Simulations were also carried out assuming the emissivity of all the walls of 0.9 instead of 0.7. It was found that the changes in both the radiative and convective heat losses were less than 4%.



(a)

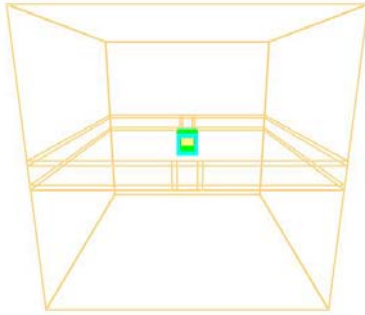


Figure 3 The receiver model in a large computational domain: (a) view from the top; (b) view from underneath.

For all cases investigated, the convective heat losses became stable in about 200s from the start of the simulation with the radiative loss stabilized even earlier at about 50s. Figure 4 and Figure 5 show the wall temperature distributions inside Receivers No. 4 and 8 at 10s, 50s and 450s from the start of the simulation. It is seen that the internal wall temperatures for both cases had stabilised in about 50s.

It should be noted that due to the unstable turbulence nature of the flow inside the upside down receiver cavity, the steady state described above is a quasi-steady state. As shown in Figure 6 and Figure 7, the convection heat losses (negative means losses through the aperture) in the time period from 300s to 400s from the start of the simulation for Receivers No. 4 and 8 are cyclic around a mean value. In this study, the total simulation time is fixed at 500s to ensure that a quasi-steady state has been reached. Each simulation took the SGI Altix roughly about 2-5 days dependent on the CPU demanding of other users.

Table 1 lists the average radiative and convective heat losses through the aperture for different receiver geometries and absorber temperatures after the system reached quasi-steady state. It is seen that in general, the convective heat loss is significantly smaller (about one order less) than the radiative loss through the aperture. This is especially true for small cavity sizes at $0.4\text{m} \times 0.4\text{m} \times 0.76\text{m}$ (depth) and $1\text{m} \times 1\text{m} \times 1\text{m}$ (depth). However, for the large cavity at $2\text{m} \times 2\text{m} \times 1\text{m}$ (depth), the convective loss becomes significant at around half the radiative heat loss.

Rec. No.	Abs. Dim. (m × m)	Apert. Dim. (m × m)	Cav. Dep. (m)	Abs. Tem (°C)	Heat Losses	
					Rad (kW)	Conv (kW)
1	1.0 × 1.0	0.8 × 0.8	1.0	550	9.5	1.6
2	1.0 × 1.0	0.8 × 0.8	1.0	600	12.1	1.9
3	1.0 × 1.0	0.8 × 0.8	1.0	650	15.2	2.2
4	2.0 × 2.0	0.8 × 0.8	1.0	600	17.1	7.4
5	0.4 × 0.4	0.2 × 0.2	0.50	850	2.4	0.12
6	0.4 × 0.4	0.4 × 0.4	0.76	700	3.0	0.23
7	0.4 × 0.4	0.4 × 0.4	0.76	800	4.5	0.30
8	0.4 × 0.4	0.4 × 0.4	0.76	900	6.4	0.38

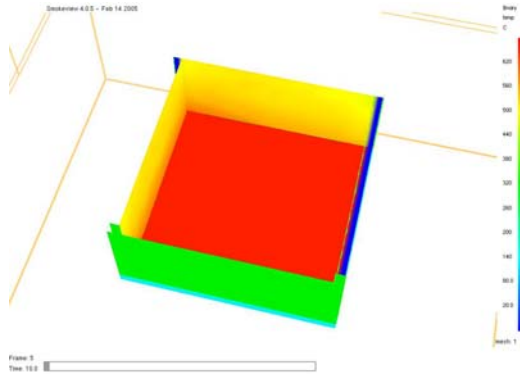
Table 1: Heat losses through the aperture for different receiver geometry and absorber operation temperatures.

Figure 8 and Figure 9 compare the velocity contour in a vertical slice through the centre of the receivers for Receivers No. 4 and 8 at 450s. It is clear that the air velocities in the large cavity are about an order higher than those in the small cavity. Figure 10 and Figure 9 compare the temperature contours in a vertical slice through the centre of the receivers for Receivers No.4 and 8 at 450s. The spill of high temperature air through the aperture is obvious in the large cavity. Consequently, due to the enhancement of air movement within the large cavity, convective heat loss through the aperture in the large receiver becomes significantly higher than in the small receiver even when the latter operates at much high absorber temperature.

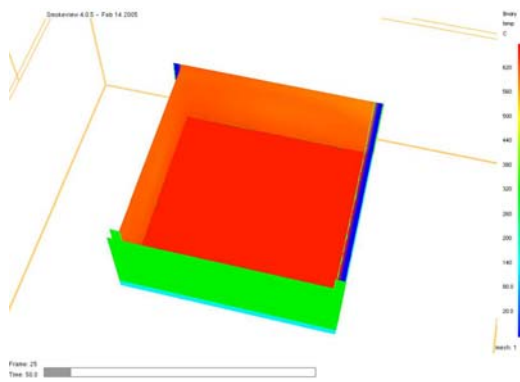
It should be noted that the FDS simulations for this study are based on the assumption that there are no conductive losses through the walls and there is no forced convection from wind. As the absorber is the only heat source in this study, the internal wall temperature must be lower than that of the absorber as shown in Figure 4 and Figure 5. Thus, the largest possible conductive heat loss through the walls is when all the internal wall temperatures are maintained at the absorber temperature. Assuming 100mm fibreglass insulation with $0.05 \text{ W/m} \cdot ^\circ\text{C}$ thermal conductivity, the conductive heat loss through the walls should be less than 400 W/m^2 for internal a wall temperature of $821 \text{ }^\circ\text{C}$.

Receiver No. 5 with $0.4\text{m} \times 0.4\text{m}$ absorber and $0.2\text{m} \times 0.2\text{m}$ aperture was designed to simulate the original receiver used by CSIRO Energy Technology (CET) at Lucas Heights. As shown in Table 1, the total heat loss through the $0.2\text{m} \times 0.2\text{m}$ aperture is estimated to be 2.5 kW. With a 100mm fibreglass thermal insulation all around the receiver walls, the conductive loss is around 0.5 kW. The effect of surrounding wind on the convective heat loss through the aperture was not modelled in this study. Clausing (1981) proposed Eq. (4) to estimate the average influx velocity V_a through the aperture with wind effect as:

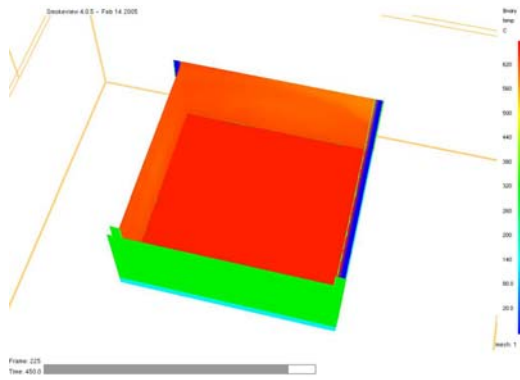
$$V_a = 0.5(V_b^2 + V_w^2)^{1/2} \quad (4)$$



(a)

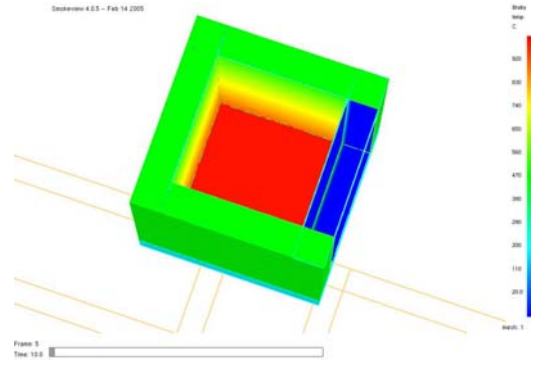


(b)

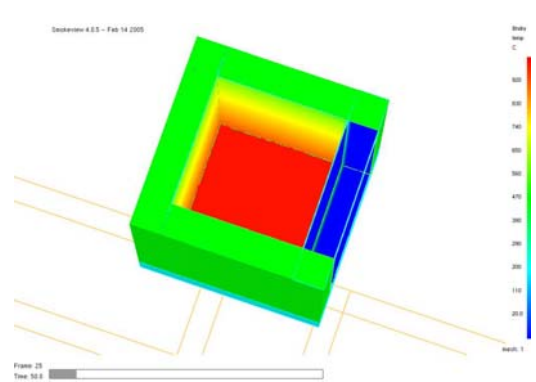


(c)

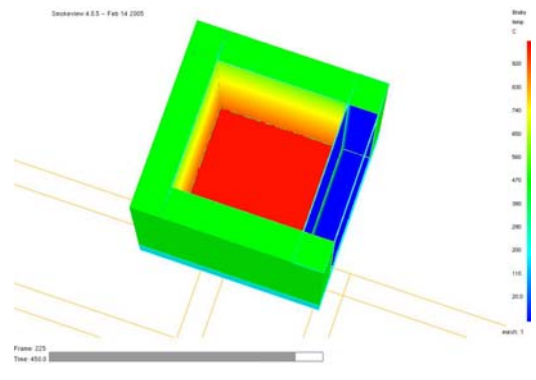
Figure 4 Wall temperature distributions inside Receiver No. 4 at 10s, 50s and 450s.



(a)



(b)



(c)

Figure 5 Wall temperature distributions inside Receiver No. 8 at 10s, 50s and 450s.

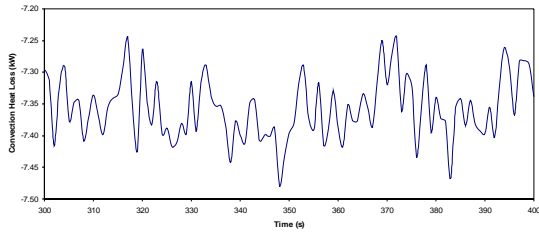


Figure 6 The cyclic convection loss through the aperture for Receiver No. 4 from 300s to 400s.

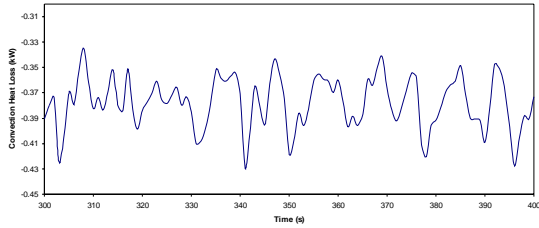


Figure 7 The cyclic convection loss through the aperture for Receiver No. 8 from 300s to 400s.

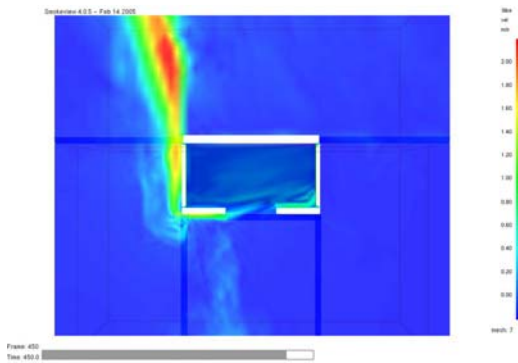


Figure 8 The velocity contour through the centre of the SCRR receiver for Receiver No. 4 at 450s.

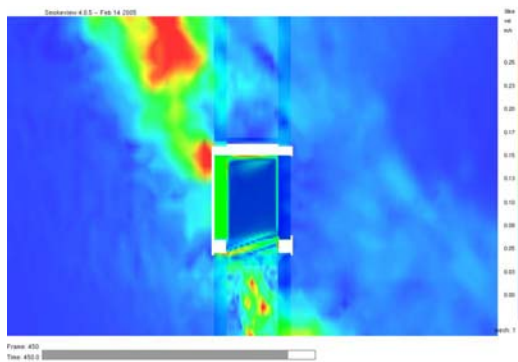


Figure 9 The velocity contour through the centre of the SCRR receiver for Receiver No.8 at 450s.

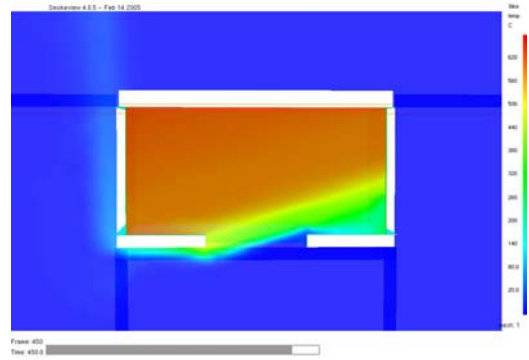


Figure 10 The temperature contour through the centre of the SCRR receiver for Receiver No.4 at 450s.

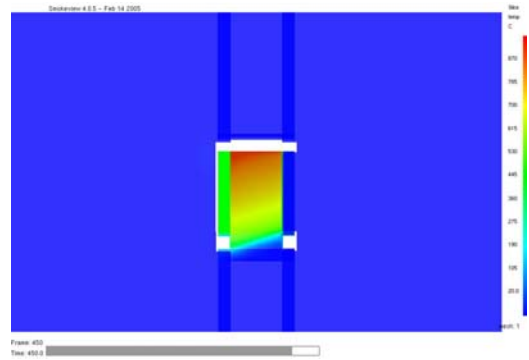


Figure 11 The temperature contour through the centre of the SCRR receiver for Receiver No.8 at 450s.

The convective loss through the aperture is roughly proportional to the average influx velocity, V_a . When the wind speed, V_w , is significantly higher than V_b , the ratio of the convective heat loss with and without the wind effect may be estimated as V_w/V_b . The yearly-averaged wind velocity in NSW is around 2.9 m/s (using Sydney airport wind data). V_b is around 0.15 m/s from the CFD modelling results for Receiver No. 5. Consequently, the convective loss with wind effect is estimated to be around 2.3 kW which is similar to the radiative heat loss as shown in Table 1. It is clear that ambient wind can have a significant impact on the convective heat loss through the aperture. The impact of wind will be relatively smaller for large cavity receivers such as Receiver No. 4 since the buoyancy induced air velocity is comparable to the ambient wind speed for large cavity receivers as shown in Figure 8.

Considering a total received solar radiation of 21 kW, the original receiver used by CET may have achieved a thermal efficiency of around 75%. This is roughly in agreement with the estimation for the original receiver and thus gives some confidence in the simulation results obtained in this study.

Modelling results for Receiver No. 8 suggest that for a total absorbed energy of 25 kW, a receiver with $0.4\text{m} \times 0.4\text{m}$ absorber and $0.4\text{m} \times 0.4\text{m}$ aperture will have 6.8kW heat loss through the aperture when operated at 900°C . Considering conductive loss of around 0.5 kW, the

thermal efficiency of Receiver No.8 is estimated to be around 71%. Similarly, Receivers No. 6 and 7 may achieve thermal efficiency of around 85% and 79% respectively. However, these thermal efficiencies were estimated without the consideration of the wind effect. As discussed above, the wind effect can be substantial for small receivers. In order to have more accurate prediction of the heat losses, especially the convective heat losses, further simulations are required to investigate the effect of wind speed on the convective heat loss through the aperture.

CONCLUSION

This paper presents the modelling results for the radiative and convective heat losses through the aperture of a cavity solar receiver at the CSIRO National Solar Energy Centre using FDS package. A modelling case designed for the original CET receiver at Lucas Heights shows that the thermal efficiency of the original receiver may be around 75% which is in agreement with the estimation for the original receiver.

In general, if there is no wind effect, convective heat loss through the aperture is much less than the radiative loss for small receivers, with this ratio increasing with aperture size. Modelling results suggested that for a total received energy of 25 kW and a receiver with 0.4m × 0.4m absorber and 0.4m × 0.4m aperture operated between 700 and 900 °C, its thermal efficiency would be in the range of 71-85% when ambient wind speed is zero.

Preliminary analysis suggested that for small cavity receivers, ambient wind may have a substantial impact on the overall heat loss from the receiver. In order to achieve high thermal efficiency, it is suggested that a small receiver should have wind guards installed to reduce the wind effect. Further simulations are required to understand the effect of wind speed on the convective heat loss through the aperture and the conduction heat losses through the walls.

REFERENCES

- CLAUSING A.M. (1981). *An Analysis of Convective Losses From Cavity Solar Central Receiver*, Sol. Energy 27, 295-300.
- CLAUSING A.M. (1983). *Convection Losses From Cavity Solar Receivers-Comparisons Between Analytical Predictions and Experimental Results*, Journal of Solar Energy Engineering 105, 29-33.
- KOENIG A.A. AND MARVIN M. (1981). *Convection heat loss sensitivity in open cavity solar receivers*, Final report, DOE contract No. EG77-C-04-3985.
- LEIBFRIED U. AND ORTJOHANN J. (1995), *Convective Heat Loss from Upward and Downward-Facing Cavity Solar Receivers: Measurements and Calculations*, J. Sol. Eng. 117, 75-84.
- MCGRATTAN, K. B, ET AL, (2005) "Fire dynamics simulator (version 4) – Technical reference guide", National Institute of Standards and Technology, USA.
- PAITONSURIKARN S. AND LOVEGROVE K. (2002). *Numerical Investigation of Natural Convection Loss in Cavity Type Solar Receivers*. In Proceedings of Solar 2002 - Australian and New Zealand Solar Energy Society, Newcastle, Australia.
- STINE W.B. AND MCDONALD C.G. (1989), *Cavity Receiver Heat Loss Measurements*, presented at ISES World Congress, Kobe, Japan.
- TAUMOEFOLAU T. AND LOVEGROVE, K. An Experimental Study of Natural Convection Heat Loss from a Solar Concentrator Cavity Receiver at Varying Orientation. In Proceedings of Solar 2002 - Australian and New Zealand Solar Energy Society, Newcastle, Australia.